DIELECTRIC CHARACTERISATION OF FOAMED CONCRETE FOR DENSITY AND COMPRESSIVE STRENGTH EVALUATION

CHONG CHIA HSING

**A project report submitted in partial fulfilment of the
requirements for the award of Bachelor of Science
(Hons.) Physics**

**Lee Kong Chian Faculty of Engineering and Science
Universiti Tunku Abdul Rahman**

April 2019

DECLARATION

I hereby declare that this project report is based on my original work except for citations and quotations which have been duly acknowledged. I also declare that it has not been previously and concurrently submitted for any other degree or award at UTAR or other institutions.

Signature :

Name : Chong Chia Hsing

ID No. : 1600730

Date : 12th April 2019

APPROVAL FOR SUBMISSION

I certify that this project report entitled **"DIELECTRIC CHARACTERIZATION OF FOAMED CONCRETE FOR DENSITY AND COMPRESSIVE STRENGTH EVALUATION"** was prepared by **CHONG CHIA HSING** has met the required standard for submission in partial fulfilment of the requirements for the award of Bachelor of Science (Hons.) Physics at Universiti Tunku Abdul Rahman.

Approved by,

Signature	:	
Supervisor	:	
Date	:	

Signature	:	
Co-Supervisor	:	
Date	:	

The copyright of this report belongs to the author under the terms of the copyright Act 1987 as qualified by Intellectual Property Policy of Universiti Tunku Abdul Rahman. Due acknowledgement shall always be made of the use of any material contained in, or derived from, this report.

ACKNOWLEDGEMENTS

I would like to thank everyone who had contributed to the successful completion of this project. I would like to express my gratitude to my research supervisor, Dr. Lee Kim Yee and Mr. Phua Yeong Nan for their invaluable advice, guidance and enormous patience throughout the development of the research.

In addition, I would also like to express my gratitude to my loving parents and friends who had helped and given me encouragement.

ABSTRACT

This thesis reports on the dielectric characterization of the lightweight foamed concrete and the relation of the three variables: density, dielectric constant, and compressive strength. The mathematical model used for the dielectric characterization of the concrete is Jonscher model and the goodness of fit of this model with the measurement is high with the R-square value reaching as high as 0.9 and above. The relationship between density and dielectric constant is simple linear equation. On the other hand, the mathematical relation between density with compressive strength and dielectric constant with compressive strength show a power-law relation with the power value reaching 3.89 and 2.4 respectively. It should worth noting that this is a cursory study for its related field and further exploration should focus on the development in the variety of mathematical models that could be used in the dielectric constant conversion as the model used in this study is capacitance model only. In addition, the software or programming of the instrument could also be improved with the transferring of control to computer. Lastly, the other structural variables of lightweight foamed concrete could be included in the analysis.

TABLE OF CONTENTS

CHAPTER

LIST OF TABLES

LIST OF FIGURES

LIST OF SYMBOLS / ABBREVIATIONS

MUT	Material Under Test
CUT	Concrete Under Test
CDC	Complex Dielectric Constant
VNA	Vector Network Analyser
LAN	Local Area Network
PC	Personal Computer
NI	National Instrument
CS	Compressive Strength
FC	Foamed Concrete

LIST OF APPENDICES

CHAPTER 1

INTRODUCTION

1.1   General Introduction

This report is divided into 5 chapters with the chapter 1 giving an introduction to the whole of the study with its objectives and aims. Chapter 2 will be discussing the concepts and theories used to conduct the experiments.

On the other hand, chapter 3 consist of the methodology of the study where the steps of the experiment conducted and programming that are done will be stated with the aim of reproducibility of experiment in mind. As for chapter 4, it is the results and discussions obtained from the experiment. Lastly, the chapter 5 will be stating the conclusion and the recommendation for future work which means the possible development of the related project from this work.

There are 4 major components for this study: the models used for open-ended coaxial probe; the models used for the dielectric characterization of concrete; the instrument programming and connection setup for measurement; the foamed concrete theory and preparation. However, the foamed concrete preparation and theory will be stated briefly as it is not the focus of the study. The models and theory for dielectric constant concrete will be stated in literature review while the instrument setup will be included in methodology.

1.2   Importance of the Study

This research can provide the civil engineers data and information about the performances of the foam concrete and metal sand mixed concrete for the better design of the building construction especially in the effect and propagation of the electromagnetic signals throughout the building.

The parameter of interest is the complex dielectric constant or permittivity.

$$\varepsilon = \varepsilon' - j\varepsilon'' \qquad\qquad (1\text{-}1)$$

where

ε' = real value of the complex dielectric constant (CDC) which relate to energy storage

ε''= imaginary part of the CDC which relate to loss or attenuation.

The investigation of the dielectric constant and loss factor of the concretes can help determined its propagation and shielding effect of the electromagnetic waves respectively. In turn, this help determine the effectiveness of the electronics in the room e.g. mobile devices receiving the 4G(frequency) or 3G(frequency) signal from their respective mobile carrier plans and Wi-Fi internet connection. (Chung, et al., 2017)

The success of this study could help interior design and civil engineers or architectures reduce their limitation on the construction and design of building regarding the shielding of the wireless signal for telecommunication. (Sandrolini, et al., 2007)

1.3 Problem Statement

There is no working model for the foamed concrete in the dielectric properties and subsequently there is no analysis for its relation between different performance indicators or parameters and the permittivity characteristics of foamed concrete.

Thus, by obtaining the relevant data on its permittivity characteristics and performance parameters which is compressive strength, it is hoped that it could reveal or aid in the discovery of its usage in construction or more. In addition to frequency response of signal, it also begged the question of changing power or magnitude of signal in relation to the stated effect for the material characterization of foamed concrete. Thus, the CDC obtained with the changing frequency and power or magnitude of the electromagnetics wave in transmission help test the correlation of performance parameter and dielectric constant.

The stated problem can help tackle the question for the best suited electromagnetics (EM) wave to be used for the telecommunication. However, as the technology progress, the telecommunication moves further into the higher frequency range. Thus, the higher frequency responses from this study can shed light on the transmission of EM wave in foamed concrete.

1.4   Aims and Objectives

The aim of the study is to investigate the dielectric characteristics of the foamed concrete with its relation to other performance indicators, for example, the compressive strength and shielding effectiveness.

The experimental objectives that need to be fulfilled for the achievement of the stated aims are to determine the CDC for both the real and imaginary part using the measurements of S-parameter for magnitude and phase in response of frequency and power. In addition, the compressive strength test will also be done along with the density determination.

In addition to the results-oriented objectives, the methodological objective is to achieve the connection and control via Local Area Network (LAN) cable with the use of MATLAB. This in turn means the successful use of SCPI command for the control of the instrument and may ultimately lead to a development of a software for the non-destructive testing of foamed concrete.

1.5   Scope and Limitation of the Study

The circumscribed region of study is limited by the theoretical models that could be applied to the measurement and also the limit of the frequency spectrum generated by the instrument.

The models that will be used consist of two stages. The first stage is the calculation of dielectric constant from the S-parameter which involves the models for the open-ended coaxial probe. On the second stage, the models are derived for the dielectric characteristics for the Foamed Concrete (FC). The specifics and types of the models will be discussed in chapter 2.

Other than the limitation imposed by the instruments and the mathematical models, it is also limited by the samples as the composition is made and prepared by the civil engineering department, the control of the composition and constituent ratio is not available. Thus, the construction of model to relate compressive strength and dielectric constant might face difficulties with the limited variation of parameters.

The scope of the study are also limited to only applying the known mathematical models of probe and models of permittivity of concrete to the foamed concrete. The coefficients for the models are mostly determined with curve fitting method using MATLAB while the methods or mathematical formula for the curve fitting is obtained and adapted from the paper by Chung. (Chung, et al., 2017)

CHAPTER 2

LITERATURE REVIEW

2.1   Introduction

The models and theory for the dielectric constant and foamed concrete will be discussed in this section and each of the topics of interest had been separated into each section. This section will be divided into 7 section with titles of Introduction, Foamed Concrete, Dielectric Measurement, Open-Ended Coaxial Probe, Frequency Dependence Models for Complex Permittivity, Density and Compressive Strength, and Summary.

2.2   Foamed Concrete

Foamed concrete (FC) is a low-density concrete with cellular structure in the concrete which is created from the foaming agent mixed in together with fine sand, cement, water and pozzolans.

Apparently, the FC is known for its fire resistance, thermal insulation and sound absorbance due to cells in the concrete created by the foams or air bubbles. In addition, the good workability of the FC also make it a good choice for the use filling and moulding of the concrete. (Amran, et al., 2015)

2.3   Dielectric Measurement

There are two methods for the measurement of electromagnetic properties of material which are non-resonant and resonant method. However, only the non-resonant method will be considered. This is because that the resonant method require the enclosure of the material under test (MUT) in the waveguide chamber for the measurement of the perturbation of the wave in order to obtain the quality factor and resonant frequency.

By considering the application of the technique on the construction or industry, the resonant method is not as widely applicable than the non-resonant method in term of mobility and the size of the test subject in construction site. In addition to the stated restriction, within the non-resonant method, there are also two criteria which are the reflection method and the reflection/transmission method. It is also been deemed more flexible and mobile to use the reflection method as it only involves one probe.

Moreover, the reflection method also have two variants which are the open reflection method and the shorted reflection method. In compliance with the name, non-destructive testing of the material, the open reflection method is used as the shorted reflection method require the extraction (destructive) of the sample to be inserted into the shorted end of the coaxial probe as shown in Figure 2-2. (Chen, et al., 2004)
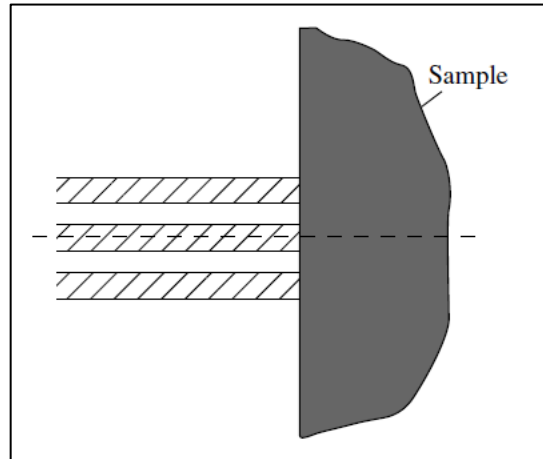
Figure 2-1: Coaxial open-circuit reflection.
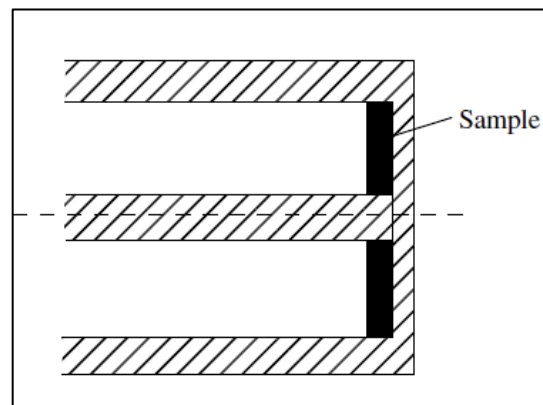
Figure 2-2: Coaxial short-circuit reflection.

Thus, given how the restrictions on the applicability and the nature of the samples, the open-ended coaxial probe is the method chosen to conduct the measurement of dielectric constant. The theory, equations and calibrations needed for the method are discussed in the next section.

2.4 Open-Ended Coaxial Probe

The open-ended coaxial probe used in the study is adopted from a previous study done by K. O. Chin. The inner and outer radii are $a = 1.5mm$ and $b = 5mm$ respectively. The geometry of the probe is shown in Figure 2-3.
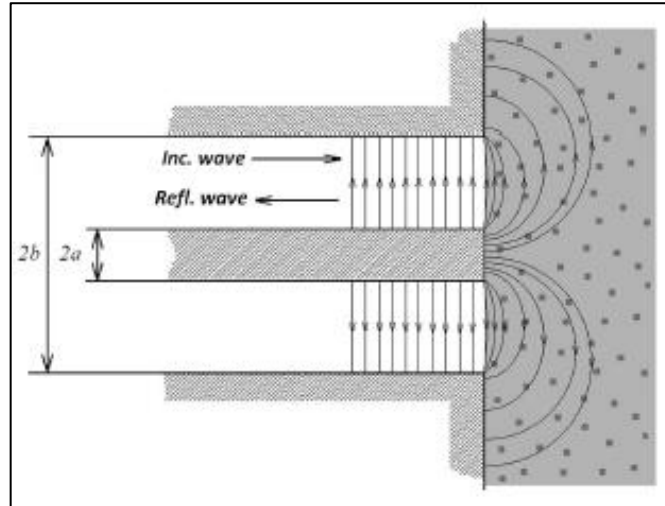
Figure 2-3: Geometry of the flanged open-ended coaxial probe.

As for the connector for the coaxial probe to the VNA port, it is a type N male connector. (Chin, 2018)

2.4.1 Models

There are four mathematical models that could be used for the conversion of the S-parameter measured from the instrument VNA to the dielectric constant. The models are capacitance model, antenna model, virtual line model, and rational function model. (Bérubé & Ghannouchi, 1996)

2.4.1.1 Capacitance Model

This model considers the sample measured as a capacitor with capacitance related to the CDC of MUT. The concept can be shown in Figure 2-4.
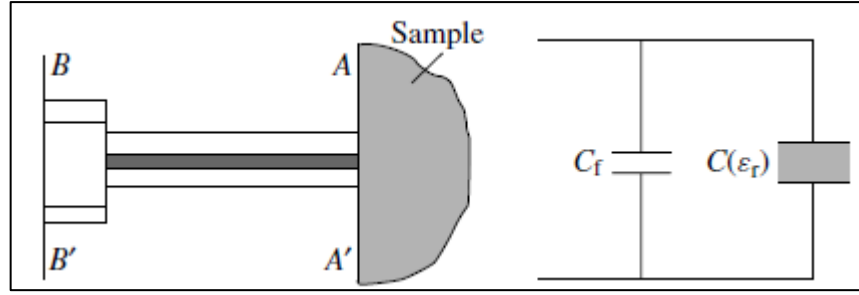
Figure 2-4: Coaxial probe terminated with a sample and its equivalent circuit.

The equation derived for this model in determining CDC is given as:

$$\varepsilon_r = \frac{1 - \Gamma^*}{j\omega Z_0 C_0 (1 + \Gamma^*)} - \frac{C_f}{C_0} \tag{2-1}$$

with the two parameters C_f and C_0 to be determined from a known CDC sample, for example, deionized water or methanol and air. The equation for the two parameters are:

$$C_0 = \frac{1 - |\Gamma_{diel}^*|^2}{\omega Z_0 \left(1 + 2|\Gamma_{diel}^*| \cos(\Phi_{diel}) + |\Gamma_{diel}^*|^2\right) \varepsilon_{diel}''} \tag{2-2}$$

$$C_f = \frac{-2|\Gamma_{diel}^*| \sin(\Phi_{diel})}{\omega Z_0 \left(1 + 2|\Gamma_{diel}^*| \cos(\Phi_{diel}) + |\Gamma_{diel}^*|^2\right)} - \varepsilon_{diel}' C_0 \tag{2-3}$$

where ε_{diel}' and ε_{diel}'' are the real and imaginary part of the CDC of the calibration standards.

2.4.1.2 Antenna Model

Next, the stated model is also called the radiation model. (Chen, et al., 2004) So, in addition to the capacitance model of the sample, a resistance is also at the mix in parallel to the capacitance model. The equivalent circuit is shown in Figure 2-5.
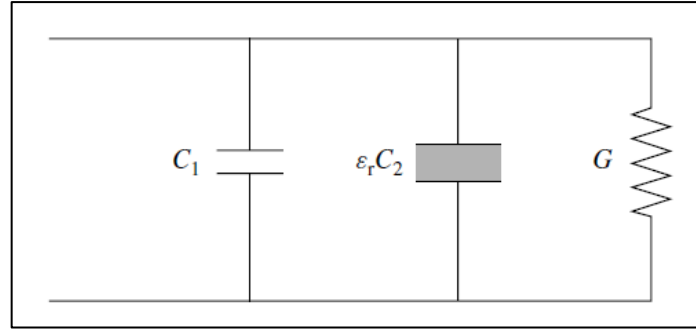
Figure 2-5: Antenna model.

The equation for this model is in the form of admittance. Thus, the measured S-parameter or reflection coefficient gamma Γ has to be converted to admittance before further calculation of CDC. The equation for the conversion is given by

$$\frac{Y}{Y_0} = \frac{1 - \Gamma}{1 + \Gamma} \tag{2-4}$$

Then, the admittance equation for the antenna model as a function of CDC is:

$$\frac{Y}{Y_0} = j\omega C_1 Z_0 + j\omega \varepsilon_r C_2 Z_0 + \varepsilon_r^{\frac{5}{2}} G(\omega, \varepsilon_0) Z_0 \tag{2-5}$$

$$\frac{Y}{Y_0} = K_1 + K_2 \varepsilon_r + K_3 \varepsilon_r^{\frac{5}{2}} \tag{2-6}$$

The coefficients K_1, K_2, and K_3 are to be determined using three standard samples with known CDC, for example, deionized water, methanol, air, and a short. With the obtained values for the coefficients, the CDC can be obtained by solving the polynomial equation given by equation (2-6).

2.4.1.3 Virtual Line Model

This model considers the EM wave permeated the MUT as an extension of the virtual coaxial line and this is modelled with the admittance and CDC of the MUT. The Figure 2-6 shows the visualization of the model.
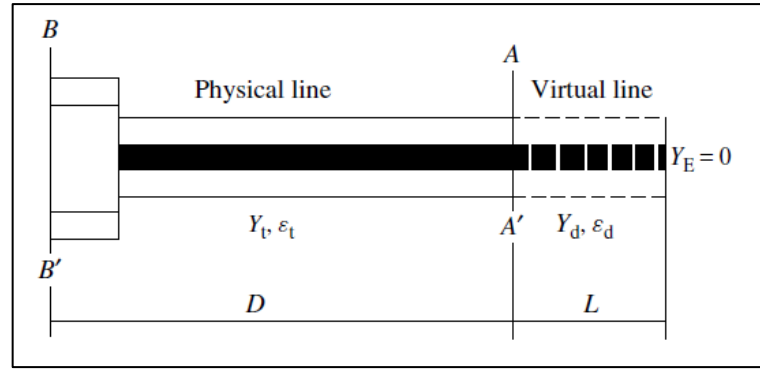
Figure 2-6: Virtual line model.

The CDC obtained for the MUT using this model will be:

$$\varepsilon_d = \frac{-jc\sqrt{\varepsilon_t}}{2\pi f L} \cdot \frac{1 - \Gamma_m e^{2j\beta_t D}}{1 + \Gamma_m e^{2j\beta_t D}} \cdot \cot\left(\frac{2\pi f L \sqrt{\varepsilon_d}}{c}\right) \qquad (2\text{-}7)$$

where the parameters with the subscript d represents the parameters for the virtual line while the subscript t goes for the coaxial probe. β parameter is propagation constant while D and L are the coefficients that needed to be determined from known standards which is similar to previous 2 models.

However, due to the lengthy and redundant process of the calculation plus the exclusion of this model for the use of obtaining the CDC from the S-parameter, this part of D and L calculation will excluded unless the other models are successfully implemented in the subsequent experiment. Then, this model will be further expanded.

2.4.1.4 Rational Function Model

A rational function model (RFM) is a rational function which is a ratio of the polynomial function given as:

$$f(x) = \frac{a_n x^n + a_{n-1} x^{n-1} + \cdots + a_2 x^2 + a_1 x + a_0}{b_n x^n + b_{n-1} x^{n-1} + \cdots + b_2 x^2 + b_1 x + b_0} \qquad (2\text{-}8)$$

The rational function model has the advantage of accommodating a wide range of shape and it has an excellent extrapolation to the outside of the data domain and still matches the theoretical values. (NIST, 2013)

The equation of the RFM for the CDC of the material are developed by Stuchly, Sibbald, and Anderson and it is expressed as

$$\frac{Y}{Y_0} = \frac{\sum_{n=1}^{4}\sum_{p=1}^{8}\alpha_{np}(\sqrt{\varepsilon_r})^p(j\omega a)^n}{1 + \sum_{m=1}^{4}\sum_{q=0}^{8}\beta_{mq}(\sqrt{\varepsilon_r})^q(j\omega a)^m} \tag{2-9}$$

where the α_{np} and β_{mq} are the coefficients to be determined and the values can be obtained from the paper by Stuchly, Sibbald and Anderson for all the fitted coefficient which is obtained from 56 dielectric constants measurement done with twenty normalized frequencies.

The CDC of MUT can then be solved using the following equation with the use of the coefficient α_{np} and β_{mq}:

$$\sum_{i=0}^{8}(b_i - Yc_i)\sqrt{\varepsilon_r}^i = 0 \tag{2-10}$$

with

$$b_p = \sum_{m=1}^{4}\alpha_{mp}(j\omega a)^m, \quad (p = 1, 2, \dots, 8) \tag{2-11}$$

$$b_0 = 0 \tag{2-12}$$

$$c_q = \sum_{m=1}^{8}\beta_{mp}(j\omega a)^m, \quad (q = 1, 2, \dots, 8) \tag{2-13}$$

$$c_0 = 1 + \sum_{m=1}^{8}\beta_{m0}(j\omega a)^m \tag{2-14}$$

The equation (2-10) will generate a polynomial equation and with the coefficient obtained from equations (2-11) to (2-14). The roots of the polynomial equation is solved to find the CDC.

There is a limitation to this model and it can only be used to find the CDC within the ranges: $(1 \leq \varepsilon' \leq 80)$, $(-80 \leq \varepsilon'' \leq 0)$, and $(1 \leq f \leq 20\ GHz)$. However, the RFM can be used in different frequency band with the coefficients α and β redefined for any prescribed frequency range using known dielectric materials. (Stuchly, et al., 1994)

2.4.2 Calibrations

Calibration are needed to transform the reference plane from the input of the port at the VNA (BB' plane) to the open-ended coaxial probe (AA' plane). This is because all the models stated previous, except the virtual line model, are modelled with the reflection coefficient or the admittance measured at AA' plane.

The S-parameter or reflection coefficient measured at BB' and AA' planes would have a phase difference of 2θ and the equation relating the parameters are shown as:

$$\Gamma^*_{A-A'} = \Gamma^*_{B-B'}e^{j2\theta} \tag{2-15}$$

where $\Gamma^*_{A-A'}$ and $\Gamma^*_{B-B'}$ are the complex reflection coefficient measured at the AA' and BB' planes respectively.

The relation of the phase at both planes with 2θ is given by:

$$2\theta = \Phi_{A-A'} - \Phi_{B-B'} \tag{2-16}$$

with $\Phi_{A-A'} = \angle\Gamma^*_{A-A'}$ and $\Phi_{B-B'} = \angle\Gamma^*_{B-B'}$. Given that the probe is in the air, an expression is obtained for the angle or phase of the complex reflection coefficient at the AA' by Bérubé and Ghannouchi with the use of the theoretical expression for $C_f + C_0$, formulated by Gajda and Stuchly, and the equations from capacitance model. The expression is given as:

$$2\theta = -4.76\omega Z_0\varepsilon_0(b - a) - \Phi_{B-B'}. \tag{2-17}$$

The specifics and derivation will have to refer to the paper (Bérubé & Ghannouchi, 1996) and (Gajda & Stuchly, 1983). The reason for skipping or simplifying the discussion is that the calibration that will be done in this study will use the built-in calibration function of the VNA instrument and it is done with three standards: open, short, and matched load (OSM).

As can be seen from the three standard calibration, it is different than the use of only open or air calibration from the previous discussion. The open calibration is done by exposing the end of the probe to air and the short is done with the use of a conducting metal plate pressed to the probe. Besides that, the matched load calibration could be exemplified as calibrating in tap water. However, in this study, the calibration will be done with the use of calibration kit ZV-Z132 and this can only bring the plane of reference to the coaxial cable. In order to calibrate to the end of the coaxial probe, another set of open air S_{11} data will be used to normalize and move the plane of reference to the desired position.

Other than the calibration done to move the reference plane from port to probe, there is also calibration done for the calculation of the CDC by determining the constants in the equations (2-1), (2-6), and (2-7) except for the RFM. It is reported by Bérubé and Ghannouchi that the deionized (DI) water serves as a better calibration standard than methanol for capacitance and virtual line models. However, the antenna or radiation model is not considered as it requires three calibration standards and all three of standards (air, DI water, and methanol) are used in it. Any addition or changes to other known CDC materials, for comparison, are not considered as it increases the errors and uncertainty of measurement. (Bérubé & Ghannouchi, 1996)

2.5   Frequency Dependence Models for Complex Permittivity

There are three models that will be looked into and these models are similarly used by Chung et al for the dielectric characterization of Chinese standard concrete. The models are first-order exponential model, Debye model, and the Jonscher model.

2.5.1   First-Order Exponential Model

The equation for this model is given by:

$$\varepsilon_r'(f) = K exp(-bf) + C \qquad\qquad (2\text{-}18)$$

where

b = time constant in seconds

C = final value

$K + C =$ Initial value

Although it is given in the paper and will be conducted in this study, the first-order exponential model is not as accurate fit for the dielectric characterization of concrete compared to the other two models. It is rather used to indicate the exponential decay nature of the dielectric constant for the concrete. In addition, the model also does not provide equation for the imaginary value of the CDC. (Chung, et al., 2017)

2.5.2 Debye Model

The Debye model is a special case of dipolar relaxation. Thus, the assumption had been made here that the particles in foamed concrete are dipolar in response to the incoming electromagnetic wave. Although, the assumption made seems far-fetched to the actual condition of the heterogeneous nature with multitude of multipoles moments for the FC, however, the general trend of excitation and relaxation for the net polar particles of FC still follow, as we assumed.

The equations for the Debye model are given by:

$$\varepsilon_r'(f) = \frac{\varepsilon_{static} - \varepsilon_\infty}{1 + (2\pi f \tau)^2} + \varepsilon_\infty \qquad (2\text{-}19)$$

$$\varepsilon_r''(f) = \frac{\varepsilon_{static} - \varepsilon_\infty}{1 + (2\pi f \tau)^2} 2\pi f \tau \qquad (2\text{-}20)$$

where ε_{static} and ε_∞ are the relative dielectric constant at the limits of low and high frequency spectrum.

In addition to the mentioned Debye model, there is an extension of the Debye model (extended Debye model) with an addition of conductivity term at the imaginary part of CDC which is used by (Sandrolini, et al., 2007). The equation for the real and imaginary part of CDC is given as

$$\varepsilon_r'(\omega) = \varepsilon_\infty + \frac{\varepsilon_{static} - \varepsilon_\infty}{1 + (2\pi f \tau)^2} \qquad (2\text{-}21)$$

$$\varepsilon_r''(\omega) = \frac{\varepsilon_{static} - \varepsilon_\infty}{1 + (2\pi f \tau)^2} 2\pi f \tau + \frac{\sigma_{dc}}{\omega \varepsilon_0} = \frac{\sigma_{eff}(\omega)}{\omega \varepsilon_0} \qquad (2\text{-}22)$$

where σ_{dc} and σ_{eff} are the dc and effective electrical conductivity respectively. The values of ε_{static}, ε_∞, τ, and σ_{dc} are determined by fitting the curve to the measurement data.

2.5.3   Jonscher Model

Jonscher model is an improvement on the Debye model where the assumption about the permanent dipolar is made to all the particles in the concrete. The Jonscher model distinguished four criteria of polarization: electronic polarization due to electrons of atom, ionic polarization which is between anion and cation, dipole polarization, and the space charge or interfacial polarization which is due to the migration of the charged particles. (Bourdi , et al., 2008)

The CDC equation for the model is given by

$$\varepsilon_e(\omega) = \varepsilon_\infty + \varepsilon_0 \chi_e(\omega) - i\frac{\sigma_{dc}}{\omega} \qquad (2\text{-}23)$$

All the mentioned polarization are all represented as electric susceptibility in the Jonscher model as shown:

$$\varepsilon = \varepsilon_0\big(\chi_{electronic} + \chi_{ionic} + \chi_{dipolar} + \chi_{interfacial}\big) \qquad (2\text{-}24)$$

where the susceptibility for each polarization are specified with the description in the subscript. However, in the Jonscher model (2-23) all the susceptibilities are grouped into one susceptibility, χ_e to simplify the equation. The combined susceptibility is expressed by the Jonscher universal dielectric response

$$\chi_e(\omega) = \chi_r \left(\frac{\omega}{\omega_r}\right)^{n-1} \left[1 - i\cot\left(\frac{n\pi}{2}\right)\right] \qquad (2\text{-}25)$$

where n is an empirical constant, χ_r is the real part of susceptibility and ω_r is an arbitrary chosen reference frequency.

Substituting the equation (2-25) into (2-23) and with some simple algebraic manipulation, the real and imaginary part of CDC is expressed as

$$\varepsilon_r'(\omega) = \chi_r \left(\frac{\omega}{\omega_r}\right)^{n-1} + \varepsilon_\infty \tag{2-26}$$

$$\varepsilon_r''(\omega) = \chi_r \left(\frac{\omega}{\omega_r}\right)^{n-1} \cot\left(\frac{n\pi}{2}\right) \tag{2-27}$$

where the three parameters n, χ_r, and ε_∞ can be determined by taking an arbitrary two frequency point ω_1 and ω_2. The calculation are

$$n = \frac{\ln\left[\frac{\sigma_r(\omega_1)}{\sigma_r(\omega_2)}\right]}{\ln\left(\frac{\omega_1}{\omega_2}\right)} \tag{2-28}$$

$$\chi_r = \frac{(\varepsilon_{r2}' - \varepsilon_{r1}')}{\left(\frac{\omega_2}{\omega_1}\right)^{n-1} - 1} \tag{2-29}$$

$$\varepsilon_\infty = \varepsilon_{r1}' - \chi_r \tag{2-30}$$

where $\varepsilon_{r1}' = \varepsilon_r'(\omega_1)$ and $\varepsilon_{r2}' = \varepsilon_r'(\omega_2)$.

2.6   Density and Compressive Strength

The compressive strength (CS) is a measure of the maximum pressure applicable to the CUT and the test is done by hydraulic compression testing machine. The mathematical model for the CS as a function of density ρ is adapted from Chung and his/her team study and it is given by

$$f_{cs}'(\rho) = a(\rho)^b \tag{2-31}$$

where the a and b are the empirical coefficient to be determined through curve fitting method.

On the other hand, the real part of CDC as a function of ρ and f is modelled as

$$\varepsilon_r'(\rho, f) = c\rho + d \tag{2-32}$$

where c and d are the regression coefficients to be determined.

An equation for the CS as a function of dielectric constant and frequency as given by:

$$f_{cs}'(\varepsilon_r', f) = (\varepsilon_r')^r + A \tag{2-33}$$

where the r and A are again required same curve fitting determination. (Chung, et al., 2017)

2.7 Errors and Discrepancies

In addition, there is also uncertainty contributed by the variation of temperature for the VNA as mentioned by Komarov in the experiment on sea ice, the VNA is placed in a heated enclosure to ensure the constancy of the ambient temperature for the instrument. (Komarov , et al., 2016)

Moreover, the surface of the concrete under test (CUT) is uneven and thus the air gap also will result in some discrepancies in the values measured for the CDC. This can be solved with the use of time-gating to eliminate the undesired data in the frequency spectrum. Further discussion will be conducted in the data analysis section.

2.8 Summary

In summary, there are four open-ended coaxial probe models and three models for the CDC characterisation of the foamed concrete. It is reported that the RFM gives an accurate results of CDC within the range of 2-5 GHz and the virtual line model gives the best accuracy over a wide range of frequency for both real and imaginary part of CDC while the antenna model come second to the accuracy of virtual line model. On the other hand, the capacitance gives the least accurate results of CDC (error $\geq$ 5%) for both the real and imaginary part. (Bérubé & Ghannouchi, 1996)

As for the best approximate of the CDC characteristic as function of frequency, it is the Jonscher Model while the least satisfying fit is the first-order exponential

model. The Debye model has similar curve with the first-order exponential model as can be seen from the study done by (Chung, et al., 2017).

The argument for the validity of the Debye model is that the effect from the electronic and ionic polarization is negligible due to high relaxation frequency (10^{15} Hz and 10^{13} Hz, respectively) compare to the operating frequency of the study. Moreover, the interfacial polarization has low relaxation frequency of around 1-100 kHz and thus the Debye model approximation is valid for the operation between the relaxation frequencies of the other polarization components.

CHAPTER 3

METHODOLOGY AND WORK PLAN

3.1   Introduction

In this section, the steps and procedures for performing the experiment are stated. The aim of this chapter is so that the reader could be able to perform the experiment from the instruction given in this section. Thus, the information might seem patchy due to the pieces of information that could be obtained from the surrounding or the instrument itself. As for the data analysis and coding, the complete code file will be added at the appendix. However, only pieces or small section of the codes will be discussed in the section for the ease of reading and more logical flow of words.

3.2   Experimental Setup for S_{11} Parameter Measurement

There are only four hardware components required for the setup of the experiment which are the open-ended coaxial probe, Vector Network Analyser (VNA), Local Area Network (LAN) cable, Personal Computer (PC). Figure 3-1 shows the experiment setup.
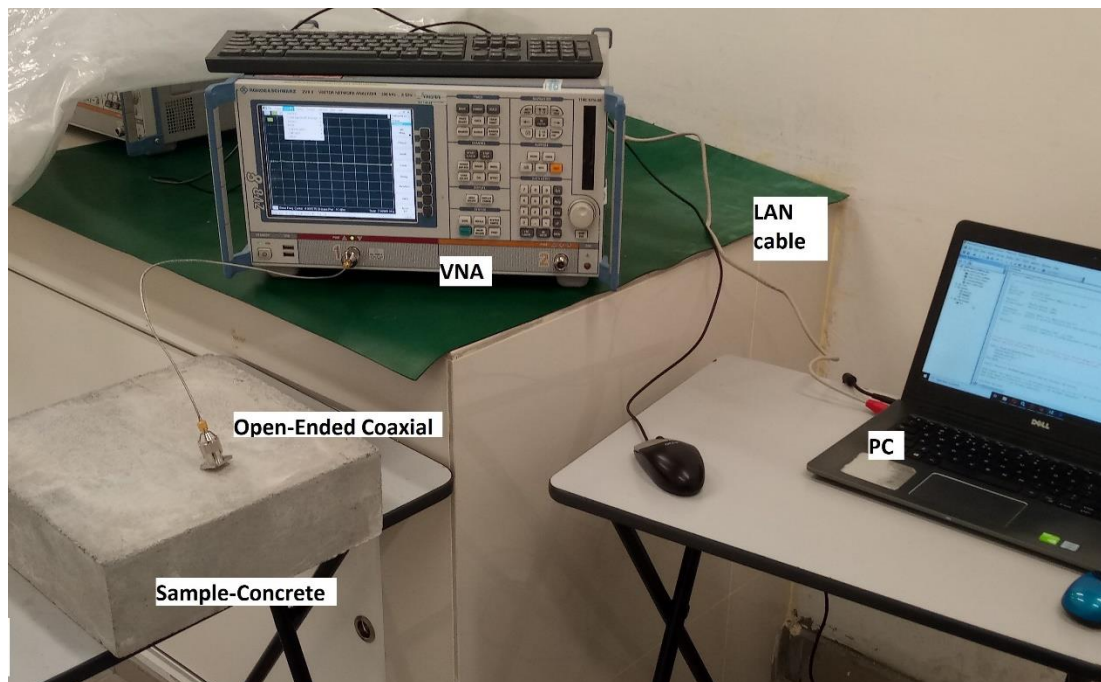

Figure 3-1: Experiment Setup.

The VNA model is R&S ZVB8 Vector Network Analyzer with 2 ports and the frequency range of the instrument is from 300 kHz to 8 GHz. In the next two subsections, the connection to PC will be discussed and follow up with the measurement procedure which formed the complete operation of the experiment.

3.2.1   Remote Control of VNA via LAN

The remote control of VNA with the use of LAN cable require the installation of the National Instrument (NI) driver which can be downloaded from the official website of NI and MATLAB. After the software installation and hardware connection of LAN cable to PC, the instrument is connect to the PC via TCP/IP connection. In order for the connection to be established, the TCP/IP address has to be set to the same number address manually.

The setting for the address can be reached by first opening the "Control panel" then proceed to the "Network and Internet" option, followed by clicking the "Network and Sharing Center", then, click the "Change adapter settings" at the sidebar where another window will popped up showing two options: "Ethernet" and "Wi-Fi". Clicking on the "Ethernet" will lead eventually to the properties of the network and IP address can then be entered for the option "Internet Protocol Version 4 (TCP/IPv4)" and the same go for the instrument. ("Control panel" > "Network and Internet" > "Network and Sharing Center" > "Change adapter settings" > "Ethernet" > "Internet Protocol Version 4 (TCP/IPv4)")

However, for the purpose of simplicity and convenient, the settings on both ends of PC and instrument for the IP address are set to automatic and the IP address is obtained from the hardware information for the instrument. The IP address obtained here is 169.254.32.166. This string of number will be needed in the programming section.

The connection can be verified by opening up the NI MAX that had been install and check the connection in the device section or a SCPI can be sent to the instrument to query a respond.

3.2.2   Measurement Procedure

The process of measurement will be done through the use of Excel file with macro function using the Visual Basic codes that are prepared by the previous student. (Chin, 2018) Figure 3-2 shows the excel file that used for the measurement.
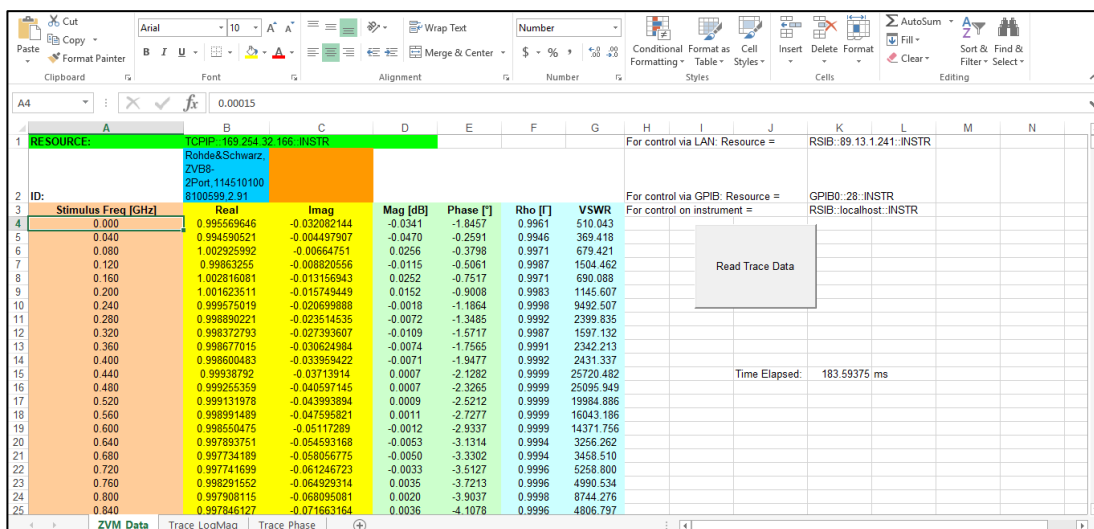
Figure 3-2: Macro used for the measurement.

Before the measurement, the sample, a $10cm \times 10cm \times 10cm$ concrete block, is marked for measurement on its six surfaces (top, bottom, and four sides surfaces) as in Figure 3-3. The top and bottom surface of the sample are labelled A and B respectively while the sides are labelled C, D, E, and F.
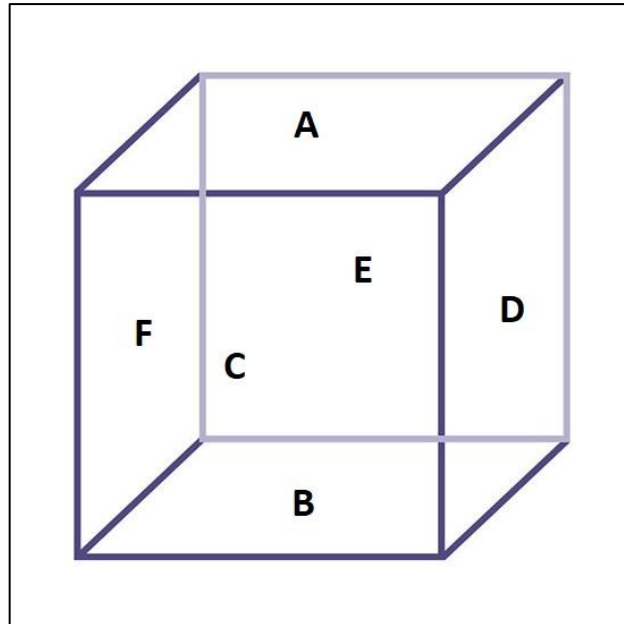
Figure 3-3: FC sample geometry and partition.

The measurement of S_{11} parameter is done on all 6 faces. After converting the 6 sets of S_{11} parameter to dielectric constants, the results would be the average of the dielectric constant of all six surfaces of the concrete block. This singular results will represent the concrete block.

Next, the coaxial probe is calibrated with the calibration kit ZV-Z132 and the connector option is set to PC 3.5 mm in the VNA window software. Then, twist the coaxial cable (after taking off the coaxial probe) onto the open, short, and match end of the calibration kit as shown in Figure 3-4.

Figure 3-4. Calibration kit.

During the measurement, the probe is pressed against the surfaces on each section while the macro button in the excel file is pressed to initiate the sweep and acquiring the data.

There are 10 sets of data that will be compared and analysis for the dielectric constants and each corresponding to a lightweight foamed concrete block.

.

3.3 Compressive Strength Measurement

The brand of the compression test machine used in this study is Unit Test Scientific Sdn. Bhd. (UTS). The machine used is custom made machine for compressing block/cube concrete structure.

The machine is shown in Figure 3-5. Before operating the machine, it is best to consult the lab assistance first. The operation of the machine is quite simple. First, the machine is switched on with the button at the position 1 in the figure. Then, specifications (dimensions, weight) of the concrete block that need to be tested is inserted into the machine with the use of the number pad at position 4.

Afterward, the block is inserted between the pistons which is located at position 6 and then the air-lock level at position 5 at the right side of the machine, which is out of sight from the figure, is tightened to prevent the air from escaping out of the piston. The bottom piston will then be risen with a green button at position 3 so that the block is firmly clamped between the pistons. Once the block is clamped between the pistons, it should be reminded that the zero error reading from the pressure need to be eliminated with the option 'Null' in the system.

After all this is done, the lever at position 2 can be pushed up and the process of compression test will begin. The process will automatically stopped once the block is crushed and the result will be shown on screen like Figure 3-6. The crushed concrete block can then be disposed and the piston is swept clean, then a new cycle will begin with a different concrete block.

Figure 3-5. Compression Test Machine.

Figure 3-6. Compression Strength of Block with 4.07 MPa.

3.4 Data Analysis and Coding

In this section, the discussion will be about how to follow through with the data acquisition and handle with the data from beginning to the end. Thus, the first thing or data that we need to look at is the initial S_{11} parameter with its corresponding frequency data.

After the acquisition, the data are extracted with the use of

```
frequency = xlsread('0dBm_surf1','ZVM_Data','A4:A204');
gamma_surf1 = db2mag(xlsread('0dBm_surf1','ZVM_Data','D4:D204'));
phase_surf1 = xlsread('0dBm_surf1','ZVM_Data','E4:E204');
```

where the frequency, reflection coefficient or S_{11} parameter in magnitude ratio dimension, and the phase of the S_{11} parameter are extracted with the name frequency, gamma_surf1, and phase_surf1 respectively. This could be seen in the APPENDICES C: Code Files.

Then, the data are converted into complex dielectric constant (CDC) using the capacitance model equation. The CDC are then write into a new excel file and the figure or graph generated are saved in MATLAB.fig format. The code writing excel file and saving figure are

```
xlswrite(filename,A,sheet,xlRange);
savefig('die_diff_surf.fig');
```

After the obtaining CDC, the data are needed for the Jonscher modelling and the curve fitting function is needed for this purpose and the code is

```
[x1] = lsqcurvefit(fun,x0,xdata,ydata1);
[f1,gof1] = fit(density,eps1,'poly1');
```

where the lsqcurvefit stands for least square curve fitting which it could be used for the curve fitting custom define nonlinear equation while fit code function is more restricted with the equation option. However, it is suffced for linear equation fitting.

From here onward, the data analysis mainly consists of curve fitting with majority usage of the two mentioned curve fitting codes. However, the goodness of fits statistics could be obtained with the use of built in Curve Fitting Toolbox 3.5.5 in MATLAB.

3.5   Summary

In summary, the connection of laptop to VNA makes convenient the data collection process although it is still far from completely remote control as some setting or specifications are setup manually on the instrument. On the other hand, the data analysis is more complicated and redundant with the coding and mathematical function needed for the curve fitting process. As for the compressive strength test, it would be best to be guided by a senior or lab assistance but it is easy to handle after one trial.

CHAPTER 4

RESULTS AND DISCUSSIONS

4.1 Introduction

In this chapter, the general structure of the discussion will follow the flow of data from the initial acquisition of the S_{11} parameter to the correlation of the variables with the use of mathematical models. The variables that will be discussed are the density, dielectric constant, and the compressive strength.

4.2 Conversion of S_{11} Parameter to CDC

As known from the chapter methodology, the S_{11} parameter is obtained from the use of excel macro. The data converted to complex dielectric constant (CDC) with the use of capacitance model. The other three models are not use and only capacitance model is used due to its simplicity. The MATLAB code file that is used in this part is shown in appendix.
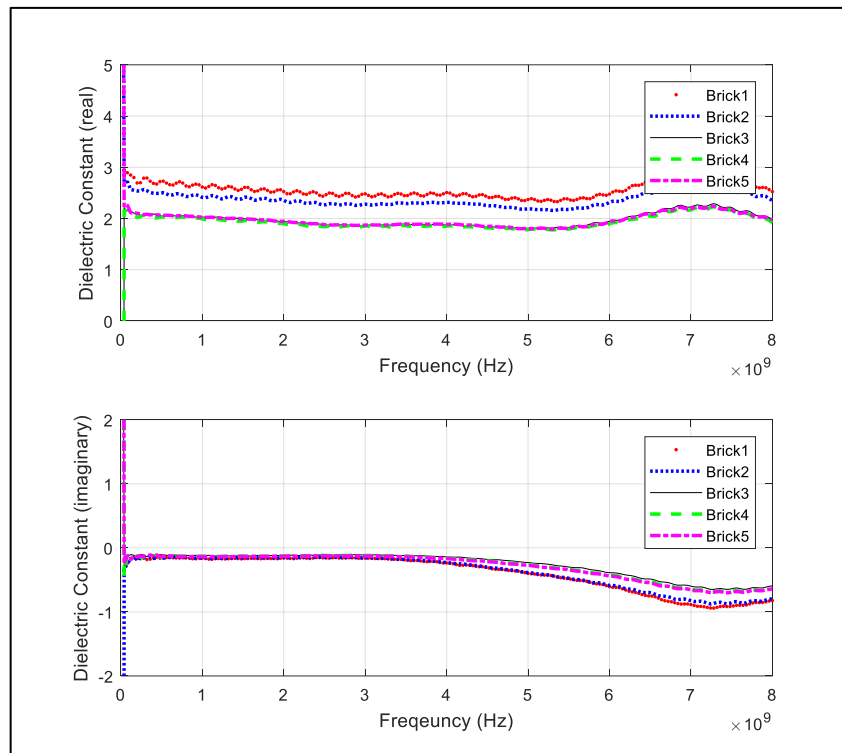

Figure 4-1.The complex dielectric constant of Brick 1 to Brick 5 (top-real & bottom-imaginary).

Figure 4-1 shows that the complex dielectric constant (CDC) for the lightweight foamed concrete. The top graph is the real part of the CDC while the bottom one is the imaginary which it is usually associated with the loss. The data is arranged so that the Brick 1 has the highest density and decreases down the numbering of the bricks. It shows that the Brick 1 has highest dielectric constant (real part of CDC) and followed by the Brick 2 while the Brick 3, 4, and 5 seem to have a same dielectric constant. It could also be seen that the same trend is reflected on the imaginary part of CDC.
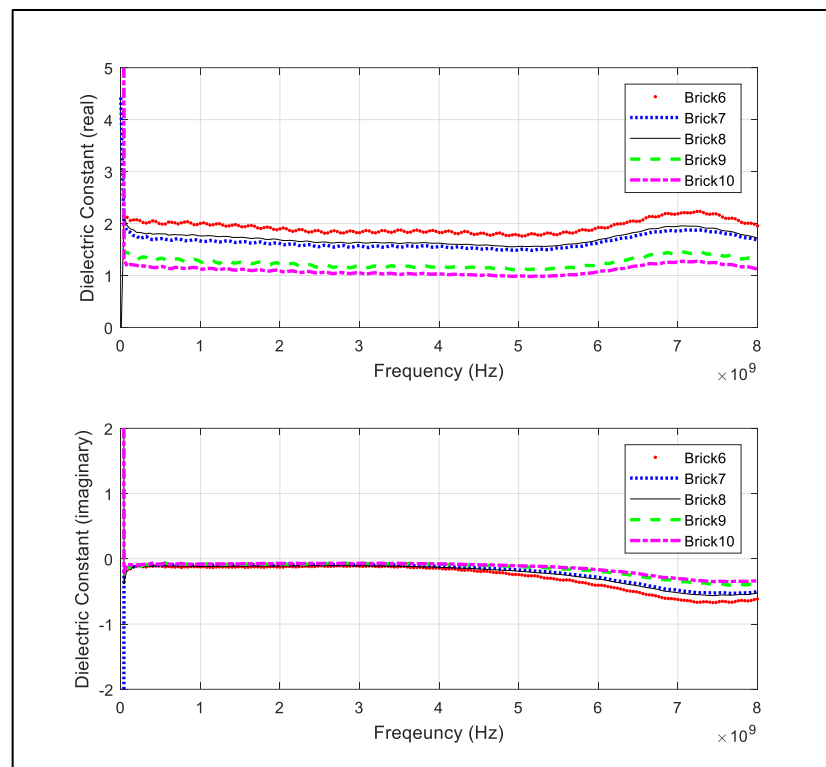
Figure 4-2.The complex dielectric constant of Brick 6 to Brick 10 (top-real & bottom-imaginary).

Figure 4-2 shows the same data set but for Brick 6 to Brick 10. It is arranged with descending order of density as mentioned. The arrangement for this group of data is obvious with Brick 6 on top followed by Brick 8 then 7, 9 and 10. Generally, the dielectric constant varies with density but in this group of data there is an outlier which are Brick 7 and 8. These two data seem to switch position in contradiction to the trend. The observed trend is similarly reflected in its imaginary part of CDC.

4.3   Jonscher Model

After obtaining the conversion to CDC, the real part of the CDCs are modelled with the use of Jonscher model for the curve in respond of the frequency. The imaginary part is of no interest in this section and so on. The equation used is shown in the previous chapter (Equation (2-26)) and the MATLAB code file used is located in appendix.

There are two parts in the processing of the Jonscher model. The first is the modelling of the whole spectrum from 0 to 8 GHz which will not be included in this section (but located in appendix) while the second part is the modelling of just 0 to 5 GHz. The reason behind such move is that the section after 5 GHz for the real part of the CDC is fluctuating and does not show the plateau nature of the model. Thus, it might generate a lot error and would jeopardize the rest of the analysis. In addition, the 0 to 5 GHz has enough data sets and it shows a nice curve fit for later analysis.
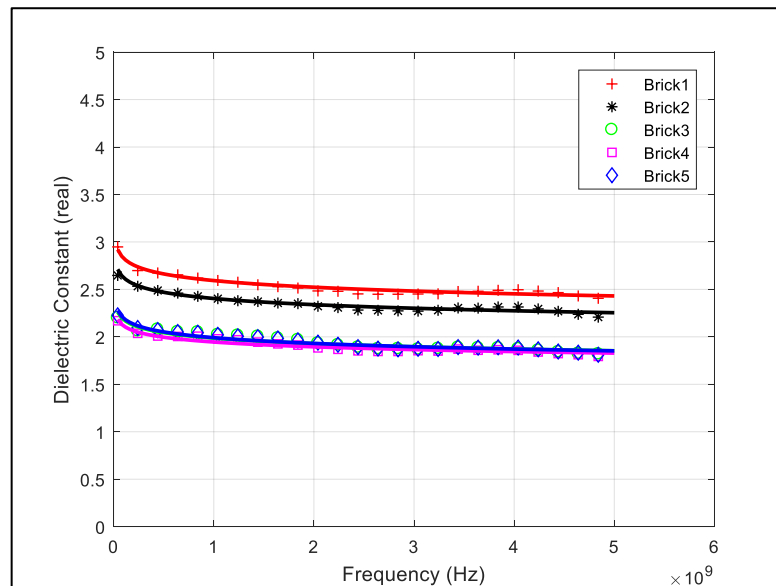

Figure 4-3: Dielectric characterization of lightweight foamed concrete via curve fitting to measure data using the Jonscher model for Brick 1 to Brick 5.
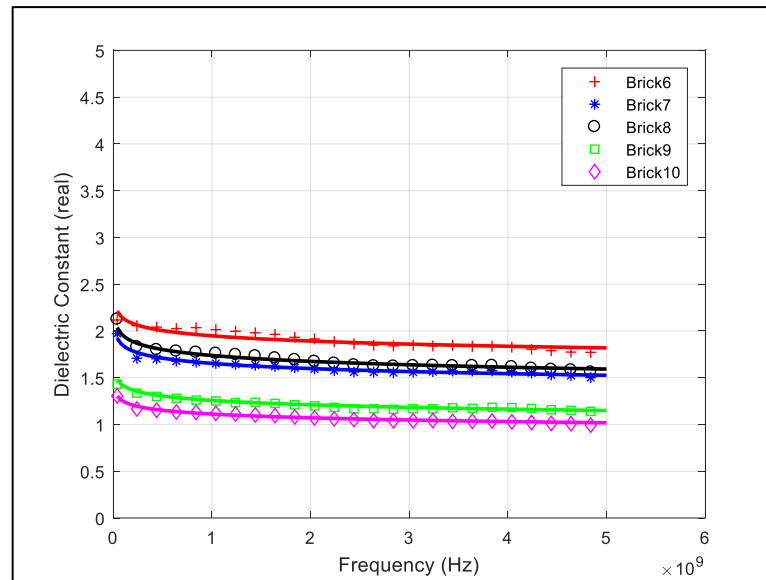
Figure 4-4: Dielectric characterization of lightweight foamed concrete via curve fitting to measure data using the Jonscher model for Brick 6 to Brick 10.

Figure 4-3 and Figure 4-4 show the curve fitting result of the Jonscher model. The three fitted parameters: χ_r, n, and ε_∞; will be used in the calculation of dielectric constant for five fixed frequencies in the further analysis of density and compressive strength.

Table 4-1. Jonscher Model: Fitting Coefficients with $f_r = 0.05\ GHz$ and Goodness of fit for Equation (2-26).

Brick	χ_r	n	ε_∞	R^2	SSE
1	-0.619	1.130	3.533	0.9190	0.1365
2	44.580	0.998	-41.890	0.8973	0.1287
3	100.700	0.999	-98.560	0.8443	0.1514
4	50.320	0.998	-48.110	0.9019	0.0872
5	31.270	0.997	-29.020	0.9101	0.0918
6	60.270	0.999	-58.070	0.8576	0.1310
7	16.710	0.995	-14.810	0.9342	0.0531
8	28.390	0.997	-26.370	0.9415	0.0619
9	35.290	0.998	-33.820	0.9011	0.0599
10	28.930	0.998	-27.640	0.9905	0.0431

The $sum\ of\ squares\ due\ to\ error\ (SSE)$ and $R-square\ (R^2)$ are obtained with the Curve Fitting Toolbox 3.5.5 available in MATLAB. The goodness of fits indicate a nice fit for the values within the range 0 to 5 GHz with the R-square

values keeping at the level 0.9 for almost all the data set. However, the goodness of fits for the full range frequency curve fitting are unsatisfactory. The maximum and minimum values for R-square are 0.1324 and 0.0446 respectively. The full table for the full range frequency curve fitting can be referred to in the appendix.

4.4   Relation between Compressive Strength and Density

In this section, the Equation (2-31) will be used for the analysis and the fitting coefficients or constants a and b will be determined with the same curve fitting function in MATLAB. It is found that $a = 4.71162334381702 \times 10^{-6}$ and $b = 3.89415590850977$. The results are shown in Figure 4-5 with the data point and curve.
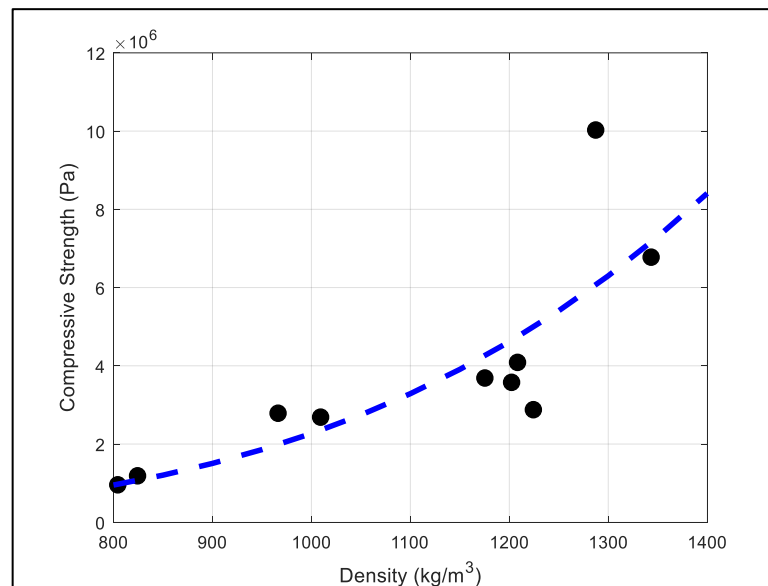
Figure 4-5. Compressive Strength versus Density of the lightweight foamed concrete.

From the figure, it could be seen that the curve is barely a nice fit. This is reflected in the goodness of fits test where $R^2 = 0.651032196$.

4.5   Relation between Dielectric Constant and Density

The relation between the dielectric constant and density are expressed as linear equation. The dielectric constant are tested on several frequency points which are 1, 2, 3, 4, and 5 GHz. Six different linear equations can be obtained for each frequency with an addition of average value for the 5 frequencies dielectric constant. The average

value is shown in Figure 4-6 and the value of constants c and d or gradient and y-intercept respectively are shown in Table 4-2.

Figure 4-6. Dielectric Constant versus Density for the average value of 1,2,3,4 & 5 GHz dielectric constants.

Table 4-2. Regression coefficients and goodness of fit for Equation (2-32).
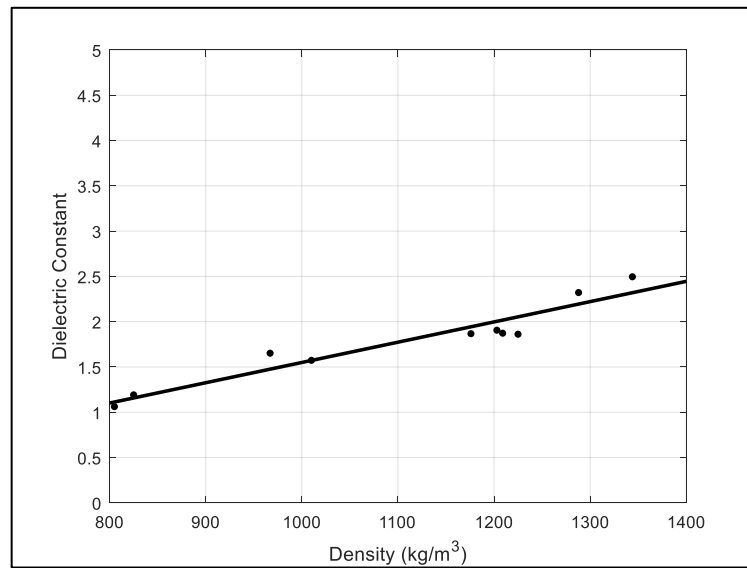
Frequency (GHz)	c	d	R^2	SSE
1	0.002287	-0.6649	0.9181	0.1526
2	0.002252	-0.6829	0.9216	0.1411
3	0.002232	-0.6932	0.9236	0.1347
4	0.002217	-0.7003	0.9250	0.1303
5	0.002206	-0.7058	0.9261	0.1269
Average	0.002239	-0.6894	0.9229	0.1369

Table 4-2 shows that the relation between density and dielectric constant are in a good linearity. The R-square values are high for each frequency points.

4.6   Relation between Compressive Strength and Dielectric Constant

For this section, the equation used are taken from the paper by K. L. Chung as mention in Chapter 2. However, it should worth noting that the derivation of equation is related to the variable w/c where in this case, the common variable is changed to density ρ. Although this poses a problem to the conceptual reasoning for its use, the other option

seems pale in comparison to the current equation in term of goodness of fit. Thus, the analysis is proceeded with said equation.

Table 4-3. Regression coefficients and goodness of fits for Equation (2-33).

Frequency (GHz)	r	A	R^2	SSE
1	2.296	-0.6542	0.7817	14.36
2	2.363	-0.5386	0.7888	13.89
3	2.410	-0.4779	0.7949	13.49
4	2.447	-0.4382	0.8001	13.15
5	2.479	-0.4093	0.8047	12.85
Average	2.396	-0.5052	0.7938	13.56

Based on Table 4-3, the curves have a quite a fit to the data with the R-square values lingering around 0.8. The fitness of the curve could be seen in Figure 4-8 while Figure 4-7 shows the trend that the curve translate upward with the increase of frequency.
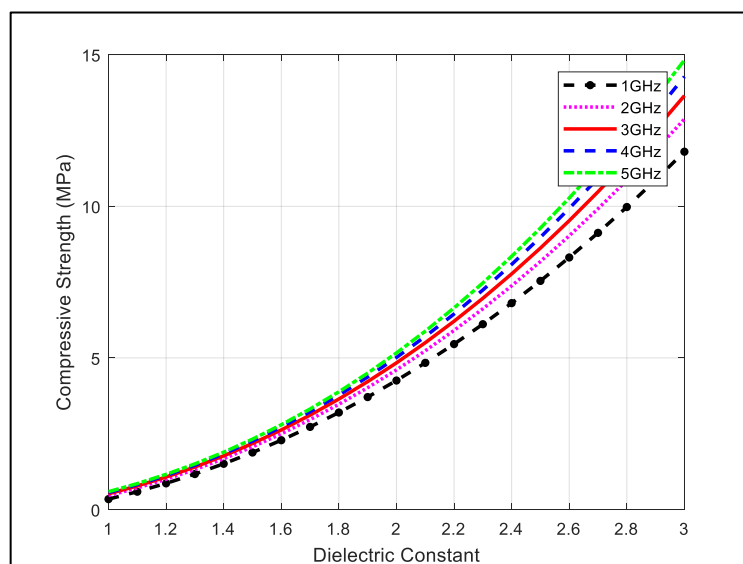
Figure 4-7. Compressive Strength versus Dielectric Constant of lightweight foamed concrete at various frequencies.
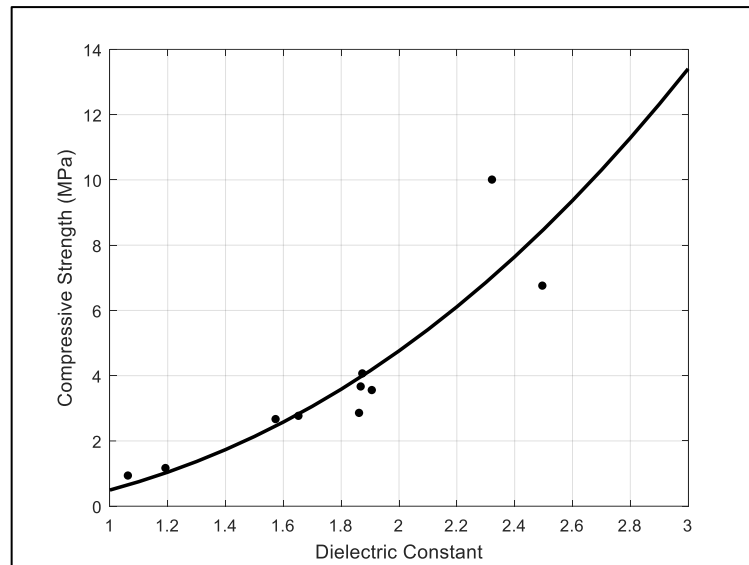
Figure 4-8. Compressive Strength versus Dielectric Constant of lightweight foamed concrete for average values of dielectric constants of various frequencies.

Figure 4-7 and Figure 4-8 show similar curve that is obtained in (Chung, et al., 2017). However, the deviation and R-square are far from the desired results as seen from the paper. It could be possible to attribute this deviation to the constancy of the w/c ratio and the instability of the lightweight foamed concrete as opposed to the hard concrete tested in the paper.

CHAPTER 5

CONCLUSIONS AND RECOMMENDATIONS

5.1 Conclusions

This study presents the dielectric characterization of the lightweight foamed concrete using the Jonscher model. This model is chosen as it is the best fitted to the dielectric constants obtained with its highest goodness of fits score out of the three models introduced.

The linear equation of the density and dielectric constant shows the best fit with the highest overall R-square value while the model for relating density and compressive strength seems to falter with a mere 0.651 R-square value. As for the equation for compressive strength and dielectric constant, it seems to stand midway through the argument.

The purpose of this study is to have a cursory exploration of the relationship between the three variables density, dielectric constant, and compressive strength. The ultimate goal was to have a deeper insight into the relationship between the variables other than the three mentioned variables and to establish a mature system for the dielectric characterization of concrete.

5.2 Recommendations for Future Work

The future of this project could be expanded in four directions or aspects. These aspects are software integration and improvement, mathematical models, mathematics amalgamation or the conceptual reasoning, and discrepancy or error compensation.

The integration of the laptop or software component into the dielectric characterization measurement system could be improved. On this part, the programming of the instrument could be its own standalone final year project with the aim of transferring the control from the vector network analyser to the laptop with the use of MATLAB and SCPI command.

As for the mathematical models, other than the mathematical models used for the conversion of dielectric constant and the dielectric characterization of concrete, the models used for the curve fitting could be improved or added upon. This could be done by adding the number variables that is involved in the process. Although the study

mainly uses two variables in the analysis for simplicity, the next step should be three variables in a single mathematical modelling or adding of new variables for more control and effect on the dielectric constant.

Thirdly, the mathematical amalgamation or the conceptual reasoning are the derivation or the understanding of how the variables are interacted with the basics law in EM theory. If the aforementioned mathematical models are more informatics and complete, the trends could shed light on how the EM wave interact in the concrete.

Lastly, the discrepancy and error compensation is more down to earth in comparison to the previous aspect, the crack and air cavity in the concrete do in certain affect the measurement. In addition, the air gap between the probe and concrete is a major concerned should be its own major project to solve the problem.

REFERENCES

Amran, Y. H. M., Farzadnia, N. & Abang Ali, A., 2015. Properties and applications of foamed concrete; a review. *Construction and Building Materials,* 101(Part 1), pp. 990-1005.

Bérubé, D. & Ghannouchi, F. M., 1996. A Comparative Study of Four Open-Ended Coaxial Probe Models for Permittivity Measurements of Lossy Dielectric/Biological Materials at Microwave Frequencies. *IEEE TRANSACTIONS ON MICROWAVE THEORY AND TECHNIQUES,* 44(10), pp. 1928-1934.

Bourdi , T., Rhazi, J. E., Boone, F. & Ballivy, G., 2008. Application of Jonscher model for the characterization of the dielectric permittivity of concrete. *Journal of Physics D: Applied Physics,* 41(20).

Chen, L.F., Ong, C.K., Neo, C.P., Varadan, V.V. and Varadan, V.K., 2004. *Microwave Electronics: Measurement and Materials Characterization.* Chichester: John Wiley & Sons Ltd.

Chin, K. O., 2018. *Development of Microwave Dielectric System for Frequency Spectrum Analysis of Lightweight Foamed Concrete,* Bandar Sungai Long: Universiti Tunku Abdul Rahman.

Chung, K.L., Yuan, L., Ji, S., Sun, L., Qu, C. and Zhang, C., 2017. Dielectric Characterization of Chinese Standard Concrete for Compressive Strength Evaluation. *Applied Sciences,* 7(2), p. 177.

Gajda, G. B. & Stuchly, S. S., 1983. Numerical Analysis of Open-Ended Coaxial Lines. *IEEE Transactions on Microwave Theory and Techniques,* 31(5), pp. 380-384.

Komarov, S.A., Komarov, A.S., Barber, D.G., Lemes, M.J. and Rysgaard, S., 2016. Open-Ended Coaxial Probe Technique for Dielectric Spectroscopy of Artificially Grown Sea Ice. *IEEE TRANSACTIONS ON GEOSCIENCE AND REMOTE SENSING ,* 54(8), pp. 4941-4951.

Macko, M., n.d. *How to use Rohde & Schwarz Instruments in MATLAB: Application Note.* 12 ed. Müchen: Rohde & Schwarz GmbH & Co. KG.

Marsland, T. P. & Evans, S., 1987. Dielectric measurements with an open-ended coaxial probe. *IEE Proceedings H - Microwaves, Antennas and Propagation,* 134(4), pp. 341-349.

NIST, 2013. *Engineering Statistics Handbook.* [Online] Available at: https://www.itl.nist.gov/div898/handbook/pmd/section6/pmd642.htm [Accessed 21 August 2018].

Rohde & Schwarz, 2016. *R&S ZVA/R&S ZVB/R&S ZVT Vector Network Analyzers: Operating Manual.* Müchen: Rohde & Schwarz GmbH & Co. KG.

Sandrolini, L., Reggiani, U. & Ogunsola, A., 2007. Modelling the electrical properties of concrete for shielding effectiveness prediction. *Journal of Physics D: Applied Physics,* Volume 40, pp. 5366-5372.

Stuchly, S. S., Sibbald, C. L. & Anderson, J. M., 1994. A New Aperture Admittance Model for Open-Ended Waveguides. *IEEE TRANSACTIONS ON MICROWAVE THEORY AND TECHNIQUES,* 42(2), pp. 192-198.

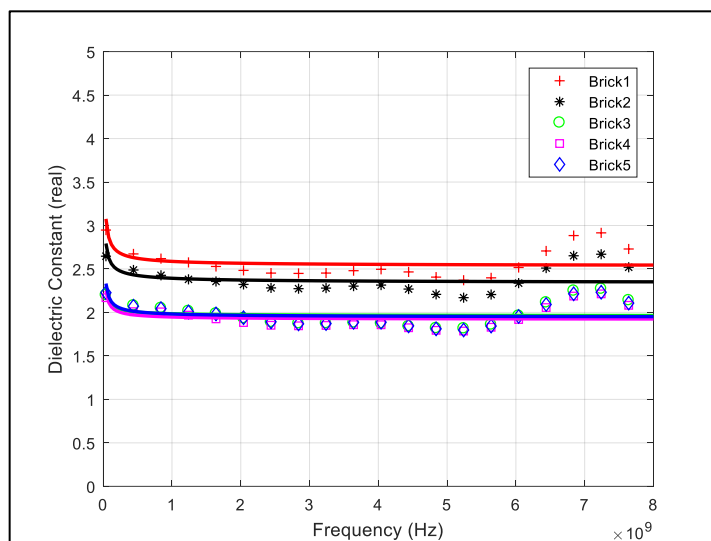**APPENDICES**

APPENDIX A: Graphs

Figure 5-1. Jonscher Model: Curve fitting for the full frequency spectrum for Brick 1 to Brick 5.
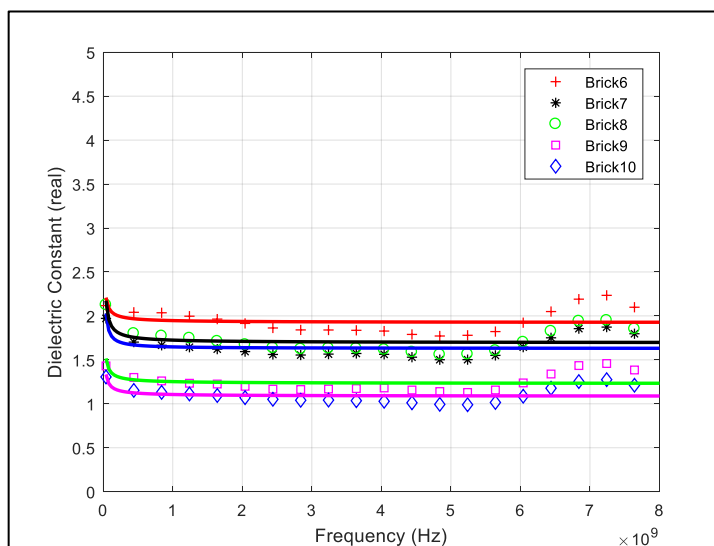

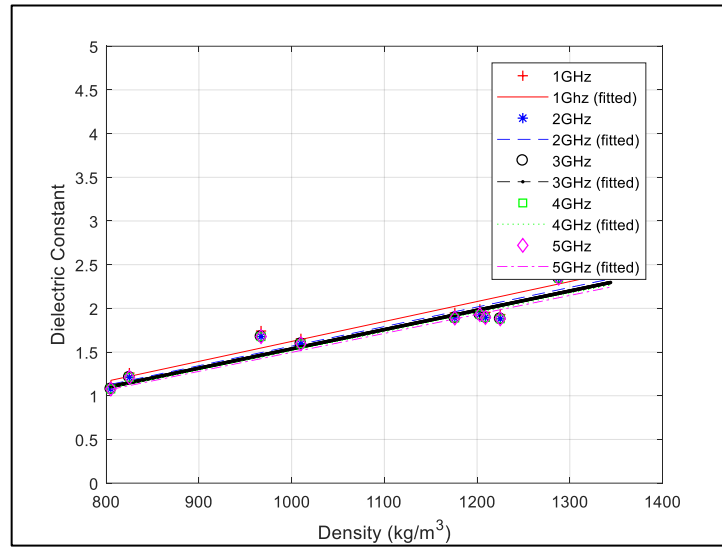Figure 5-2. Jonscher Model: Curve fitting for the full frequency spectrum for Brick 6 to Brick 10.

Figure 5-3. Dielectric constant versus Density for various frequencies.

APPENDIX B: Tables

Table 5-1. Bricks' constituent and its compressive strength.

Bricks	Egg Shell Content (%)	Density $\rho\ (\frac{kg}{m^3})$	Compressive Strength (MPa)	Water-to-Cement ratio (w/c)
1	5.0	1344	6.76	0.60
2	0.0	1288	10.01	0.68
3	7.5	1225	2.86	-
4	2.5	1209	4.07	0.60
5	0.0	1203	3.56	-
6	5.0	1176	3.67	0.60
7	5.0	1010	2.67	0.60
8	0.0	967	2.77	0.64
9	0.0	825	1.17	0.68
10	5.0	805	0.94	0.68

Table 5-2. Jonscher Model: Fitted coefficients for the full frequency spectrum curve fitting.

Brick	χ_r	n	ε_∞	R^2	SSE
1	0.465	0.286	2.533	0.1065	4.617
2	0.394	0.343	2.338	0.1083	3.358
3	0.270	0.206	1.960	0.0517	3.266
4	0.281	0.241	1.919	0.0662	2.776
5	0.333	0.288	1.943	0.0938	2.729
6	0.241	0.225	1.923	0.0446	3.067
7	0.323	0.046	1.629	0.0908	2.412
8	0.399	0.154	1.693	0.1324	2.493
9	0.242	0.219	1.229	0.0758	1.762
10	0.211	0.236	1.084	0.0782	1.306

Table 5-3. Dielectric constants at different frequency points and its average.

Brick	Density $\rho \left(\frac{kg}{m^3}\right)$	$\varepsilon_r'(1GHz)$	$\varepsilon_r'(2GHz)$	$\varepsilon_r'(3GHz)$	$\varepsilon_r'(4GHz)$	$\varepsilon_r'(5GHz)$	$\overline{\varepsilon_r'(f)}$
1	1344	2.620	2.533	2.479	2.439	2.407	2.496
2	1288	2.410	2.346	2.308	2.282	2.261	2.321
3	1225	1.929	1.880	1.852	1.832	1.816	1.862
4	1209	1.954	1.895	1.861	1.837	1.818	1.873
5	1203	1.989	1.929	1.894	1.869	1.849	1.906
6	1176	1.948	1.890	1.856	1.831	1.813	1.867
7	1010	1.652	1.595	1.561	1.538	1.520	1.573
8	967	1.741	1.676	1.639	1.612	1.592	1.652
9	825	1.259	1.211	1.182	1.162	1.146	1.192
10	805	1.117	1.077	1.054	1.038	1.025	1.062

APPENDIX C: Code Files

Capacitance Model Conversion

```matlab
%% epsilon conversion
clear all;
%% Data
frequency = xlsread('0dBm_surf1','ZVM_Data','A4:A204');
frequency = frequency*1e9;
gamma_surf1 = db2mag(xlsread('0dBm_surf1','ZVM_Data','D4:D204'));
phase_surf1 = xlsread('0dBm_surf1','ZVM_Data','E4:E204');
gamma_air = db2mag(xlsread('air(0dBm)','ZVM_Data','D4:D204'));
phase_air = xlsread('air(0dBm)','ZVM_Data','E4:E204');
omega = 2.*pi.*frequency;        %angular frequency
epsilon_0 = 8.854187818e-12;     %vacuum permittivity
b = 0.0048;                      %external conductor radius
a = 0.00145;                     %internal conductor radius
c_0 = 2.38*epsilon_0*(b-a);      %parasitic capacitance
Z_0 = 50;                        %intrinsic impedance
%% Calculation
gamma_surf1 = gamma_surf1./gamma_air;
phase_surf1 = phase_surf1 - phase_air;
gamma_complex_surf1 =
gamma_surf1.*cosd(phase_surf1)+1i.*gamma_surf1.*sind(phase_surf1);
epsilon_surf1 = (1-
gamma_complex_surf1)./(1i.*omega.*Z_0.*c_0.*(1+gamma_complex_surf1));
epsilon_real_surf1 = real(epsilon_surf1);
epsilon_imag_surf1 = imag(epsilon_surf1);
%% Display graph
figure
subplot(2,1,1);
plot(frequency, epsilon_real_surf6, '-r','LineWidth',2);
xlabel('Frequency (Hz)');
ylabel('Dielectric constant');
ylim([0 5]);
subplot(2,1,2);
plot(frequency, epsilon_imag_surf6, '-r','LineWidth',2);
ylim([-2 2])
print('dielectric_diff_surf','-dpng');
savefig('die_diff_surf.fig');
%% Averaging all six measurements
epsilon_matrix = [epsilon_surf1 epsilon_surf2 epsilon_surf3 epsilon_surf4
epsilon_surf5 epsilon_surf6];
epsilon_average = mean(epsilon_matrix,2);
epsilon_average_real = real(epsilon_average);
epsilon_average_imag = imag(epsilon_average);
figure
subplot(2,1,1);
plot(frequency, epsilon_average_real, '-k','LineWidth',2);
hold on
xlabel('Frequency (Hz)');
ylabel('Dielectric constant (real)');
ylim([0 5]);
grid on
grid minor
subplot(2,1,2);
plot(frequency, epsilon_average_imag, '-k','LineWidth',2);
hold on
xlabel('Frequency (Hz)');
ylabel('Dielectric constant (imaginary)');
ylim([-2 2])
grid on
grid minor
print('Average_dielectric','-dpng');
savefig('average_die.fig');
%% Write to Excel file
filename = 'epsilon_b1(0dBm).xlsx';
A = epsilon_average_real;
sheet = 1;
xlRange = 'B2';
xlswrite(filename,A,sheet,xlRange);
% frequency
A = epsilon_average_imag;
```

Jonscher Modelling

```matlab
%% Jonscher
clear global
filename1 = 'b1.xlsx';
sheet = 1;
xlRange = 'A3:A202';
frequency = xlsread(filename1,sheet,xlRange);
%% Dielectric
xlRange_real = 'B3:B202';
epsilon_real1 = xlsread(filename1,sheet,xlRange_real);
%% Curve fit
xdata = frequency;
ydata1 = epsilon_real1;
f_r = 0.05*10^9;
fun = @(x,xdata)x(1).*(xdata./(f_r)).^(x(2)-1)+x(3);
x0 = [1,0.1,1];
[x1] = lsqcurvefit(fun,x0,xdata,ydata1);
%% fitted curve calculation
eps_fun1 = x1(1).*(xdata./f_r).^(x1(2)-1)+x1(3);
%% Graph
figure
plot(frequency,epsilon_real1,'.r');
hold on;
plot(frequency,eps_fun1,'-r','Linewidth',2);
xlabel('Frequency (Hz)');
ylabel('Dielectric Constant (real)');
ylim([0 5]);
grid on;
legend('Brick1','Brick2','Brick3','Brick4','Brick5');
savefig('Jonscherfirst5.fig');
%% Write to Excel file
% dielectric
A = ["Brick","Chi","n","e_infty"];
filename_coef = 'Jonscherfirst5coef.xlsx';
sheet = 1;
xlRange = 'A2:D2';
xlswrite(filename_coef,A,sheet,xlRange);
A = x1;
```